Computing guided modes for an unbounded stratified medium in integrated optics

Fabrice Mahé *

April 2000

Abstract

We present a finite element method to compute guided modes in a stratified medium. The major difficulty to overcome is related to the unboundedness of the stratified medium. Our method is an alternative to the use of artificial boundary conditions and to the use of integral representation formulae. The domain is bounded in such a way we can write the solution on its lateral boundaries in terms of Fourier series. The series is then truncated for the computations over the bounded domain. The problem is scalar and 2-dimensional.

Introduction

To compute a solution for a 2-dimensional problem set in an unbounded domain, we can use artificial boundary conditions: Dirichlet, Neumann, Fourier conditions. It is the simplest way to program but it needs large computational domains in order to reduce the computing error. Moreover, it doesn't work for all the examples. We can find examples of such finite element computations for integrated optics in [13, 9].

On the other hand, we can try to write an exact condition on a boundary which can be chosen arbitrarily. Indeed, we are usually interested in knowing the solution in a small area around the center of the phenomenon. The coupling method between finite elements and an integral representation, and the localized finite element method are such numerical methods.

The coupling method between finite elements and an integral representation has been introduced by Jami and Lenoir in hydrodynamics [8]. It needs the calculation of the Green function for the 2-dimensional problem. In guided optics, this function has been determined for an homogeneous medium and a diopter, which is a medium composed of two layers with different refractive index [7]. But, for a complete stratified medium with three layers or more, this work is hard and time expensive.

The localized finite element method consists in using a series expansion of the solution in the exterior domain. This method was introduced and studied by Lenoir and Tounsi [10] in hydrodynamics, then, in guided optics, by Bonnet [1, 4] for the optical fiber with an homogeneous cladding and Gmati [7] for the diopter. For a complete stratified medium, this method leads to difficulties of the same order than the calculation of the Green function but we have adapted it in a method which is possible to use.

In fact, we present here an hybrid method between the localized finite element method and the homogeneous Dirichlet condition. Indeed, we don't need to write an exact condition on all

*Fabrice.Mahe@univ-rennes1.fr - IRMAR, Campus de Beaulieu, Université de Rennes 1, 35042 Rennes Cedex

the boundary because we can use the properties of the stratified medium. In the case of an unbounded stratified medium we know the solutions are extensive in the direction of the strata (horizontally) and well confined on the other direction (vertically). So, we choose a rectangular domain with the upper boundary parallel with the strata of the medium, writing an homogeneous Dirichlet (or Neumann) condition on the horizontal boundaries and an exact condition, coming from the localized finite element method, on the others. Contrarily to the method with a Dirichlet condition, this method allows to compute laterally extensive solutions and to study numerically structures of optical guide which couldn't be considered otherwise.

This numerical study completes the one started in [11] and is the continuation of the mathematical study which can be found in [2, 3]. In section 1 we present the problem and the mathematical results usefull to understand the method and interpret the numerical results. We give, in section 2, the study of the vertical one-dimensional problem used in the method to write the exact boundary condition. The numerical study of this one-dimensional problem is not straightforward and present a non trivial algorithm; indeed, it is in this part that the difficulty associated to the stratified medium is numerically solved. Then, we describe the numerical method in section 3. In last section, we present numerical tests which illustrate the mathematical results.

1 Modeling and mathematical results

Integrated optics is a scientific and technical field where one tries to reduce the dimensions of components guiding light waves and to lay down the maximum of components on a minimum of area. It is the optical alternative to integrated electronics for the treatment of information, like optical fibers are the alternative to electric wires for the transmission of information for large distances.

The waveguides considered here are composed of layers of different materials. These materials differ for the light propagation by their refractive index. A guide is assumed to be invariant in the propagation direction (Ox_3), see Figure 1. Then, it is completely defined by the distribution of the refractive index in a transverse section. We speak about refractive index profile and it is noted $n(x_1, x_2)$ or $n(x)$. In the transverse section, the guide appears like a compact perturbation K, the core of the guide, of a stratified medium, the cladding of the guide. The cladding is said dispersive when waves of different frequencies k propagate with different velocities.

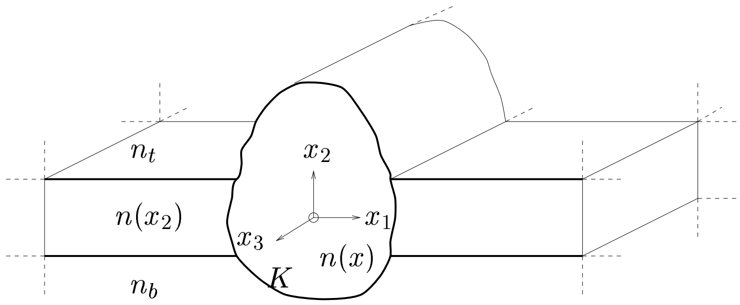

Figure 1: Stratified optical guide.

The stratified medium is supposed unbounded in the transverse directions because the dimensions of the core are small compared to the dimensions of the cladding and because we are interested in the modes guided by this device, which are waves with a transverse energy confined in a neighborhood of the perturbation. Thus, we define $n(x_1, x_2)$ as a positive function in $L^\infty(\mathbb{R}^2)$. Let

$\bar{n} \in L^{\infty}(\mathbb{R})$ be a function with positive values,

$$\bar{n} : \xi \in \mathbb{R} \longmapsto \bar{n}(\xi) \in \mathbb{R}_*^+$$

such that

$$\bar{n}(\xi) = \begin{cases} n_t & \text{if} \quad \xi > c \\ n_b & \text{if} \quad \xi < -c \end{cases}, \qquad \inf_{\xi \in \mathbb{R}} \bar{n}(\xi) > 0, \tag{1}$$

for some positive c. The values n_t, n_b play the same role and without loss of generality we choose

$$n_b \geq n_t.$$

The function n satisfies the following assumptions

$$n \in L^{\infty}(\mathbb{R}^2), \quad \inf_{x \in \mathbb{R}^2} n(x) > 0, \tag{2}$$

and there exists a compact set $K \subset \mathbb{R}^2$ such that

$$\text{for all } x = (x_1, x_2) \notin K, \quad n(x) = \bar{n}(x_2). \tag{3}$$

Let n_+ denote the essential supremum of n,

$$n_+ = \|n\|_{\infty, \mathbb{R}^2}.$$

A mode is a non trivial solution of the Maxwell equations with the following form:

$$\begin{pmatrix} \mathbb{E} \\ \mathbb{H} \end{pmatrix} (x_1 \ , x_2 \ , x_3 \ , t) = Re \left(\begin{pmatrix} E \\ H \end{pmatrix} (x_1 \ , x_2) \ e^{i(kc_l t - \beta x_3)} \right), \tag{4}$$

where $\mathbb{E}$ and $\mathbb{H}$ are the electric and magnetic fields, c_l is the speed of the light in the vacuum, k is the wave number, and β is the propagation constant of the mode which propagates with a velocity $v = \frac{kc}{\beta}$. We say that a mode is guided if it propagates without attenuation and has a finite transverse energy, that is

$$k, \ \beta \in \mathbb{R} \quad \text{and} \quad E, \ H \in (L^2(\mathbb{R}^2))^3.$$

If the transverse energy is not finite, the mode is a radiation mode. Roughly speaking a light wave propagating inside the guide is decomposed in the guided modes which are guided inside the core and the radiation modes which disperse into the cladding.

The way in which the wave propagates in the direction (Ox_3) and with respect to time is fixed by (4). The guide is invariant in this direction. Thus the problem depends only on the coordinates x_1 and x_2. Under the assumption of weak guidance (i.e. large wave number and weak variations of the index), for zero order approximation of the Maxwell system, the electro-magnetic field is transverse and each component u satisfies the scalar equation:

$$-\triangle u - k^2 n^2 u = -\beta^2 u, \quad \text{in } \mathbb{R}^2, \tag{5}$$

see for instance [1, 15, 17]. Thus the guided modes are associated with the eigenpairs (λ, u) of the unbounded operator $A_k : H^2(\mathbb{R}^2) \subset L^2(\mathbb{R}^2) \longrightarrow L^2(\mathbb{R}^2)$ depending on the positive real parameter k and defined for u in the usual Sobolev space $H^2(\mathbb{R}^2)$ by:

$$A_k \, u = -\triangle u - k^2 n^2 u$$

$(\lambda = -\beta^2)$. The operator A_k is self-adjoint, bounded from below and with non compact resolvent. The spectrum of A_k is noted $\sigma(A_k) \subset [-k^2 n_+^2, \infty[$ and consists of a continuum, the essential spectrum $\sigma_{ess}(A_k)$, and of a discrete set, the discrete spectrum $\sigma_d(A_k)$, which is the set of isolated eigenvalues of finite multiplicity. See [1, 2, 11]. The essential spectrum is given by

$$\sigma_{ess}(A_k) = [\gamma_1(k),\ +\infty[\quad \text{with} \quad \gamma_1(k) = \inf_{\substack{\varphi\in H^1(\mathbb{R})\\ \varphi\neq 0}} \frac{\displaystyle\int_{\mathbb{R}} \left\{ |\varphi'|^2 - k^2\bar{n}^2 |\varphi|^2 \right\} dy}{\displaystyle\int_{\mathbb{R}} |\varphi|^2 \ dy}.$$

See [2] for all the mathematical results. The values of the essential spectrum of A_k correspond to the propagation constants of radiation modes.

The guidance comes from differences of speed of light in the various materials with different indices (the velocity in a medium with index n_* is $v = \frac{c_l}{n_*}$). Indeed, to have guidance, the index of the material in the core must be greater than the index of the cladding. The waves propagate slower in the core and accumulate. If the greatest index is n_+ and the smallest is n_-, the velocity of the guided mode $v = \frac{kc_l}{\beta}$ lies between $\frac{c_l}{n_+}$ and $\frac{c_l}{n_-}$.

The eigenproblem (5) is equivalent to the variational formulation: find $\lambda \in \mathbb{R}$ and $u \in H^1(\mathbb{R}^2)$, $u \neq 0$, such that

$$a(k;u,v) = \lambda(u,v)_{0,\mathbb{R}^2}, \quad \text{for all } v \in H^1(\mathbb{R}^2), \tag{6}$$

where the bilinear form $a(k;.,.) : H^1(\mathbb{R}^2) \times H^1(\mathbb{R}^2) \to \mathbb{R}$ is given by: for $u, v \in H^1(\mathbb{R}^2)$

$$a(k;u,v) = \int_{\mathbb{R}^2} (\nabla u \nabla v - k^2 n^2 uv)\, dx.$$

We have necessarily $-k^2n_+^2 \leq \lambda \leq -k^2n_b^2$. We have described and computed a case in [6, 11] where $\gamma_1(k) < \lambda < -k^2n_b^2$. Here we are interested in computing the eigenpairs (λ, u) such that $\lambda < \gamma_1(k)$. These values are characterized by the min-max principle [14]

$$\lambda_1(k) = \inf_{\substack{v\in H^1(\mathbb{R}^2)\\ v\neq 0}} \frac{a(k;v,v)}{(v,v)_{0,\mathbb{R}^2}}$$

and for $m > 1$

$$\lambda_m(k) = \inf_{H_m \in \mathscr{H}_m(H^1(\mathbb{R}^2))} \sup_{\substack{v\in H_m\\ v\neq 0}} \frac{a(k;v,v)}{(v,v)_{0,\mathbb{R}^2}},$$

where $\mathscr{H}_m(H^1(\mathbb{R}^2))$ is the set of m-dimensional subspaces of $H^1(\mathbb{R}^2)$. Then

$$-k^2n_+^2 \leq \lambda_1(k) \leq \lambda_2(k) \leq \ldots \leq \lambda_m(k) \leq \ldots \leq \gamma_1(k)$$

and if $\lambda_j(k) = \gamma_1(k)$ for some $j \geq 1$ then A_k has at most $(j-1)$ eigenvalues below $\gamma_1(k)$. If $\lambda_j(k) < \gamma_1(k)$, then $\lambda_1(k), \ldots, \lambda_j(k)$ are the first j eigenvalues of A_k. Moreover the numbers $\lambda_m(k), m > 1$, can be characterized by

$$\lambda_m(k) = \sup_{v_1,\ldots,v_{m-1}\in L^2(\mathbb{R}^2)} \inf_{\substack{w\in H^1(\mathbb{R}^2), w\neq 0\\ w\in[v_1,\ldots,v_{m-1}]^\perp}} \frac{a(k;w,w)}{(w,w)_{0,\mathbb{R}^2}},$$

where $[v_1, \ldots, v_{m-1}]^\perp$ is the orthogonal complement in $L^2(\mathbb{R}^2)$ to $v_1, \ldots, v_{m-1}$. In particular when $\lambda_{m-1}(k) < \gamma_1(k)$ then

$$\lambda_m(k) = \inf_{\substack{w\in H^1(\mathbb{R}^2), w\neq 0\\ w\in[u_1,\ldots,u_{m-1}]^\perp}} \frac{a(k;w,w)}{(w,w)_{0,\mathbb{R}^2}},$$

where $u_1, \dots, u_{m-1}$ are eigenvectors associated to the eigenvalues $\lambda_1(k), \dots, \lambda_{m-1}(k)$.

We need now to report a comparison method described and used in [2]. We compare the solutions of problems stated in two subdomains of $\mathbb{R}^2$ containing K to the one stated in $\mathbb{R}^2$.

Let $a, b \in \mathbb{R}^+$ be such that $K \subset (-a, a) \times (-b, b)$. We define the two different sets

$$\begin{aligned} \Omega &= \{x \in \mathbb{R}^2; |x_2| < d\}, & (7)\\ \Omega_b &= (-a, a) \times (-d, d), & (8) \end{aligned}$$

where $d = \max(b, c)$ with c defined in (1).

Let $n \in L^\infty(\mathbb{R}^2)$ be an index function satisfying (2) and (3). On the set Ω and Ω_b we consider eigenproblems with homogeneous Dirichlet or Neumann boundary conditions.

We define the problem (P^d): find $\lambda \in \mathbb{R}$, $u \in H_0^1(\Omega)$, $u \not\equiv 0$, such that

$$a_\Omega(k; u, v) = \lambda(u, v)_{0,\Omega}, \quad \text{for all } v \in H_0^1(\Omega)$$

where the bilinear form $a_\Omega(k; u, v) : H^1(\Omega) \times H^1(\Omega) \longrightarrow \mathbb{R}$ is given by

$$a_\Omega(k; u, v) = \int_\Omega \left\{ \nabla u \nabla v - k^2 n^2 uv \right\} dx.$$

We denote by A_k^d the operator given by the spectral formulation. We define the quantities, associated with the problem (P^d),

$$\lambda_m^D(k) = \inf_{H_m \in \mathscr{H}_m(H_0^1(\Omega))} \sup_{\substack{v \in H_m \\ v \neq 0}} \frac{a_\Omega(k; v, v)}{(v, v)_{0,\Omega}}.$$

Similarly, we define (P^{dd}), A_k^{dd}, $\lambda_m^{dd}(k)$ in replacing Ω by Ω_b.

We now define the problem (P^n): find $\lambda \in \mathbb{R}$, $u \in H^1(\Omega)$, $u \not\equiv 0$, such that

$$a_\Omega(k; u, v) = \lambda(u, v)_{0,\Omega} \quad \text{for all } v \in H^1(\Omega).$$

We denote by A_k^n the operator given by the spectral formulation. As before we associate with the eigenproblem (P^n) the quantities

$$\lambda_m^N(k) = \inf_{H_m \in \mathscr{H}_m(H^1(\Omega))} \sup_{\substack{v \in H_m \\ v \neq 0}} \frac{a_\Omega(k; v, v)}{(v, v)_{0,\Omega}}.$$

In the same way we define (P^{nn}), A_k^{nn}, $\lambda_m^{nn}(k)$ in replacing Ω by Ω_b. Using the min-max principle we prove the following proposition.

Proposition 1 *Then for all $m \in \mathbb{N}^*$, $k \in \mathbb{R}_+^*$, the following holds*

$$\min(\gamma_1(k), \lambda_m^{nn}(k)) \leq \min(\gamma_1(k), \lambda_m^n(k)) \leq \lambda_m(k) \leq \lambda_m^d(k) \leq \lambda_m^{dd}(k). \tag{9}$$

2 One dimensional problem

We study in this section the vertical one-dimensional problem used in section 3 to write the exact boundary condition. It comes from the 2-dimensional equation (5) set in the domain where the function n is only dependent on x_2.

2.1 Mathematical results

A function $\bar{n} \in \mathrm{L}^\infty(\mathbb{R})$ satisfying (1) is associated with n satisfying (2) and (3). Likewise, with the problem (5) is associated the following one dimensional problem: find real numbers β and functions $\varphi \in H^2(\mathbb{R})$, $u \neq 0$, such that

$$-\frac{d^2\varphi}{dy^2} - k^2\bar{n}^2\varphi = -\beta^2\varphi, \quad \text{in } \mathbb{R}. \tag{10}$$

To solve (10) is to find the eigenpairs (γ, φ) of the unbounded operator $B_k : H^2(\mathbb{R}) \subset L^2(\mathbb{R}) \longrightarrow L^2(\mathbb{R})$ defined for $\varphi \in H^2(\mathbb{R})$ by

$$B_k\,\varphi = -\varphi'' - k^2\bar{n}^2\varphi.$$

This operator is self-adjoint, bounded from below and $\sigma_{ess}(B_k) = [-k^2n_b^2,\ +\infty[$, see [2] for all the mathematical results of this section. The eigenvalues of B_k are characterized by

$$\gamma_m(k) = \inf_{H_m \in \mathscr{H}_m H^1(\mathbb{R})} \sup_{\substack{\varphi \in H_m \\ \varphi \neq 0}} \frac{b(k;\varphi,\varphi)}{\|\varphi\|_{0,\mathbb{R}}}, \quad m \geq 1,$$

where $b(k;\varphi,\psi) = \int_{\mathbb{R}} \varphi'\psi' - k^2\bar{n}^2\varphi\psi\,dy$ and $\mathscr{H}_m(H^1(\mathbb{R}))$ is the set of m-dimensional subspaces of $H^1(\mathbb{R})$. Indeed, if $\gamma_m(k) < -k^2n_b^2$ then $\gamma_m(k)$ is the m^{th} eigenvalue of B_k, and if $\gamma_m(k) = -k^2n_b^2$ then B_k has at most $(m-1)$ eigenvalues. Moreover, if $\bar{n}_+ = n_b$ then B_k has no eigenvalue and if $\bar{n}_+ > n_b$ then $\sigma_p(B_k) \subset]-k^2n_+^2, -k^2n_b^2[$. So, we suppose now that

$$\bar{n}_+ > n_b.$$

More precisely, with $n_b > n_t$, there exists k_m such that $\gamma_m(k) = -k^2n_b^2$ for all $k \leq k_m$ and $\gamma_m(k) < -k^2n_b^2$ for all $k > k_m$. We can also give a convergence result. If there exists $0 < \eta < c$ such that

$$\begin{cases} \bar{n}(y) = \bar{n}_+ & \text{if } y \in [-\eta,\eta], \\ \bar{n}(y) < \bar{n}_+ & \text{otherwise,} \end{cases}$$

then

$$\gamma_m(k) + k^2\bar{n}_+^2 \leq \frac{m^2\pi^2}{4\eta^2} \quad \text{and} \quad \gamma_m(k) + k^2\bar{n}_+^2 \to \frac{m^2\pi^2}{4\eta^2} \text{ as } k \to \infty.$$

As we have associated A_k^d and A_k^n with A_k, we associate with B_k the two operators with compact resolvent B_k^d and B_k^n defined by

$$D(B_k^d) = H^2(I_d) \cap H_0^1(I_d), \qquad B_k^d\,u = -\frac{d^2u}{dy^2} - k^2\bar{n}^2u$$

and

$$D(B_k^n) = \{u \in H^2(I_d); u'(-d) = u'(d) = 0\}, \quad B_k^n\,u = \frac{d^2u}{dy^2} - k^2\bar{n}^2u.$$

Then we define the numbers for $m \geq 1$

$$\gamma_m^d(k) = \inf_{H_m \in \mathscr{H}_m(H_0^1(I_d))} \sup_{\substack{\varphi \in H_m \\ \varphi \neq 0}} \frac{b(k;\varphi,\varphi)}{\|\varphi\|_{0,I_d}}, \quad \gamma_m^n(k) = \inf_{H_m \in \mathscr{H}_m(H^1(I_d))} \sup_{\substack{\varphi \in H_m \\ \varphi \neq 0}} \frac{b(k;\varphi,\varphi)}{\|\varphi\|_{0,I_d}},$$

characterizing the eigenvalues of B_k^d and B_k^n. Each operator has an increasing sequence of eigenvalues tending to ∞. They give upper and lower bounds for the eigenvalues of B_k:

$$\min(\gamma_m^n(k), -k^2n_b^2) \leq \gamma_m(k) \leq \gamma_m^d(k).$$

Moreover, if $\gamma_1(k) < -k^2n_b^2$ we have $\gamma_1^N(k) < \gamma_1(k)$.

2.2 Numerical study

For the numerical study we are only interested in the case of the three layers with

$$\bar{n}(y) = \begin{cases} n_t & \text{if } y > c, \\ \bar{n}_+ & \text{if } -c < y < c, \\ n_b & \text{if } y < -c, \end{cases}$$

where $\bar{n}_+ > n_b \geq n_t > 0$. To compute $\gamma_m(k)$, we solve the equation

$$-\frac{d^2\varphi}{dy^2} - k^2\bar{n}^2\varphi = \gamma\varphi$$

successively in the intervals $]-\infty, -c[,]-c, c[$, and $]c, \infty[$, and impose the continuity of v and its derivative at $y = -c$, $y = c$. Then the eigenvalues $\gamma_m(k)$ are the solutions γ of the dispersion equation which can be written in the form

$$\tan(x) = F(x)$$

with $x = 2c\sqrt{\gamma + k^2\bar{n}_+^2} \in [0, \eta_1]$ and

$$F(x) = \frac{x\left(\sqrt{\eta_1^2 - x^2} + \sqrt{\eta_2^2 - x^2}\right)}{x^2 - \sqrt{\eta_1^2 - x^2}\sqrt{\eta_2^2 - x^2}},$$

here $\eta_1 = 2kc\sqrt{\bar{n}_+^2 - n_b^2}$, $\eta_2 = 2kc\sqrt{\bar{n}_+^2 - n_t^2}$. The function F has a pole at the point

$$x_p = \frac{2kc\sqrt{(\bar{n}_+^2 - n_t^2)(\bar{n}_+^2 - n_b^2)}}{\sqrt{(\bar{n}_+^2 - n_t^2) + (\bar{n}_+^2 - n_b^2)}}$$

and is decreasing on both intervals $[0, x_p[$ and $]x_p, \eta_1]$. Then, to get the $\gamma_m(k)$, we compute by dichotomy the intersection between a decreasing function and an increasing function on each interval where there is at most one intersection, see Figure 2.

To give an numerical illustration, we take the following data

$$\bar{n}_+ = 3, \quad n_b = 2, \quad n_t = 1, \quad c = 1, \quad k = 2, \tag{11}$$

and we compute three eigenvalues γ, see after for the values. We can deduce the eigenvectors, see Figure 2, with

$$\begin{aligned} v(y) &= C_1 e^{\alpha y} && \text{if } y \in]-\infty, -c[, \\ &= C_2 \sin(\kappa y) + C_3 \cos(\kappa y) && \text{if } y \in]-c, c[, \\ &= C_4 e^{-\delta y} && \text{if } y \in]c, +\infty[, \end{aligned}$$

where three of the constants C_1, C_2, C_3, C_4 are depending of γ and

$$\kappa = \sqrt{\gamma + k^2\bar{n}_+^2}, \quad \alpha = \sqrt{-\gamma - k^2 n_b^2}, \quad \delta = \sqrt{-\gamma - k^2 n_t^2}.$$

In the rest of the paper, to have a simpler notation, the bounded domain in the direction (Ox_2) is $I_d =]-d, d[$, a symmetrical set. It is not always the case and here we are going to consider a more general one, replacing I_d by $I_b =]-d_1, d_2[$. To compute the eigenpairs of B_k^d and B_k^n we need to distinguish three intervals dividing $[-k^2\bar{n}_+^2, \infty[$, the interval containing the eigenvalues,

$$I_1 = [-k^2\bar{n}_+^2, -k^2 n_b^2], \quad I_2 = [-k^2 n_b^2, -k^2 n_t^2], \quad I_3 = [-k^2 n_t^2, \infty[.$$

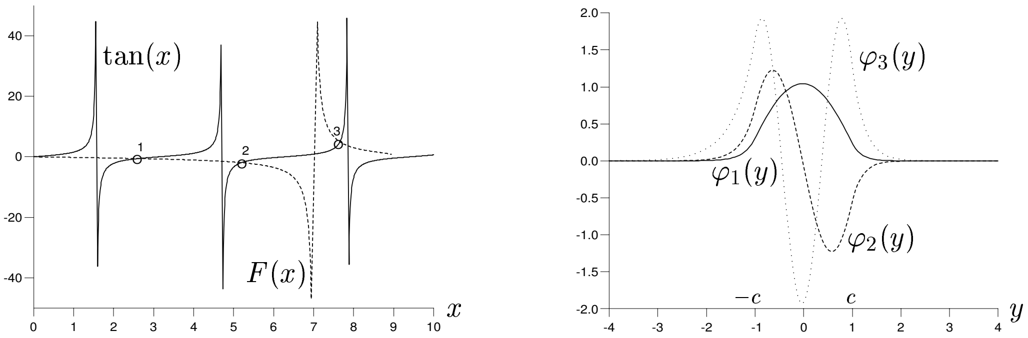

Figure 2: Curves for computing the three eigenvalues and the eigenvectors on $]-\infty,\infty[$.

Firstly, we detail the results for B_k^d. With the same method than with the unbounded domain, adding the boundary conditions $v(-h_1) = v(h_2) = 0$ and replacing the intervals $]-\infty,-c[$ and $]c,\infty[$ by $]-h_1,-c[$ and $]c,h_2[$, we get three different dispersion equations depending on the interval I_j, $j = 1,2,3$,

$$\tan(x) = F_j(x), \qquad \text{if } x \in I_j,$$

where

$$F_1(x) = \frac{x\left\{\sqrt{\eta_1^2 - x^2}\,\coth\left[\sqrt{\eta_1^2 - x^2}\,(\frac{h_1}{2c} - \frac{1}{2})\right] + \sqrt{\eta_2^2 - x^2}\,\coth\left[\sqrt{\eta_2^2 - x^2}\,(\frac{h_2}{2c} - \frac{1}{2})\right]\right\}}{x^2 - \sqrt{\eta_1^2 - x^2}\,\sqrt{\eta_2^2 - x^2}\,\coth\left[\sqrt{\eta_1^2 - x^2}\,(\frac{h_1}{2c} - \frac{1}{2})\right]\coth\left[\sqrt{\eta_2^2 - x^2}\,(\frac{h_2}{2c} - \frac{1}{2})\right]},$$

$$F_2(x) = \frac{x\left\{\sqrt{x^2 - \eta_1^2}\,\mathrm{cotan}\left[\sqrt{x^2 - \eta_1^2}\,(\frac{h_1}{2c} - \frac{1}{2})\right] + \sqrt{\eta_2^2 - x^2}\,\coth\left[\sqrt{\eta_2^2 - x^2}\,(\frac{h_2}{2c} - \frac{1}{2})\right]\right\}}{x^2 - \sqrt{x^2 - \eta_1^2}\,\sqrt{\eta_2^2 - x^2}\,\mathrm{cotan}\left[\sqrt{x^2 - \eta_1^2}\,(\frac{h_1}{2c} - \frac{1}{2})\right]\coth\left[\sqrt{\eta_2^2 - x^2}(\frac{h_2}{2c} - \frac{1}{2})\right]},$$

$$F_3(x) = \frac{x\left\{\sqrt{x^2 - \eta_1^2}\,\mathrm{cotan}\left[\sqrt{x^2 - \eta_1^2}\,(\frac{h_1}{2c} - \frac{1}{2})\right] + \sqrt{x^2 - \eta_2^2}\,\mathrm{cotan}\left[\sqrt{x^2 - \eta_2^2}\,(\frac{h_2}{2c} - \frac{1}{2})\right]\right\}}{x^2 - \sqrt{x^2 - \eta_1^2}\,\sqrt{x^2 - \eta_2^2}\,\mathrm{cotan}\left[\sqrt{x^2 - \eta_1^2}\,(\frac{h_1}{2c} - \frac{1}{2})\right]\mathrm{cotan}\left[\sqrt{x^2 - \eta_2^2}\,(\frac{h_2}{2c} - \frac{1}{2})\right]}.$$

For B_k^n we have the same expressions in replacing coth with tanh and cotan with $-\tan$. In I_1, $\gamma_m^d(k)$ and $\gamma_m^n(k)$ are approximation of $\gamma_m(k)$, while in I_2 and I_3 they give a discretization of $\sigma_{ess}(B_k)$.

Numerically, we use the same method as for the unbounded domain, but it's more complicated because it is not easy to find the intervals where there is at most one intersection, see Figure 3. In the interval I_1, F_1 as only one pole that we determine by dichotomy, and it is the same than above. We give some precisions for I_3 because it is the most complicated. Firstly, we need to find the poles of F_3. The poles and zeros of the function $x \longmapsto \mathrm{cotan}\left[\sqrt{x^2 - \eta_1^2}\,(\frac{h_1}{2c} - \frac{1}{2})\right]$ are, for $m \in \mathbb{N}$,

$$p_{m,1} = \frac{2c}{h_1 - c}\sqrt{m^2\pi^2 + (\bar{n}_+^2 - n_b^2)k^2(h_1 - c)^2},$$
$$z_{m,1} = \frac{2c}{h_1 - c}\sqrt{(m + \frac{1}{2})^2\pi^2 + (\bar{n}_+^2 - n_b^2)k^2(h_1 - c)^2}.$$

Replacing h_1 with h_2 and n_b with n_t, we get $p_{m,2}$ and $z_{m,2}$ the poles and zeros of the function $x \longmapsto \mathrm{cotan}\left[\sqrt{x^2 - \eta_2^2}\,(\frac{h_2}{2c} - \frac{1}{2})\right]$. The principle is to arrange the $p_{m,1}$, $z_{m,1}$, $p_{m,2}$, $z_{m,2}$ which define intervals where there is at most one pole of F_3. We get the poles and then between two successive poles there is one intersection between $\tan(x)$ and $F_3(x)$.

In each interval I_j we have a different expression of the eigenvectors, see Figure 4 and 5 for an illustration. We give these different expressions in the following table for B_k^d,

	I_1	I_2	I_3
J_1	$2C_1e^{-\alpha h_1}\sinh(\alpha(y+h_1))$	$C_5[\sin(\tilde\alpha y)+\tan(\tilde\alpha h_1)\cos(\tilde\alpha c)]$	$C_9[\sin(\tilde\alpha y)+\tan(\tilde\alpha h_1)\cos(\tilde\alpha c)]$
J_2	$C_2\sin(\kappa y)+C_3\cos(\kappa y)$	$C_6\sin(\kappa y)+C_7\cos(\kappa y)$	$C_{10}\sin(\kappa y)+C_{11}\cos(\kappa y)$
J_3	$2C_4e^{\delta h_2}\sinh(\delta(y-h_2))$	$2C_8e^{\delta h_2}\sinh(\delta(y-h_2))$	$C_{12}[\sin(\tilde\delta y)-\tan(\tilde\delta h_2)\cos(\tilde\delta y)]$

where $y \in J_1 =]-h_1, -c[$, $J_2 =]-c, c[$ or $J_3 =]c, h_2[$, and

$$\tilde\alpha = \sqrt{k^2n_b^2+\gamma}, \quad \tilde\delta = \sqrt{k^2n_t^2+\gamma}.$$

For B_k^n, you replace sinh with cosh and tan with $-$cotan.

We consider the same data as in (11) with

$$h_1 = 3 \qquad \text{and} \qquad h_2 = 4. \tag{12}$$

We give on the Figure 3 the graphs of the functions tan, F_1, F_2, F_3 for B_k^d. The first eigenvectors are given on Figure 4 for B_k^d and on Figure 5 for B_k^n.

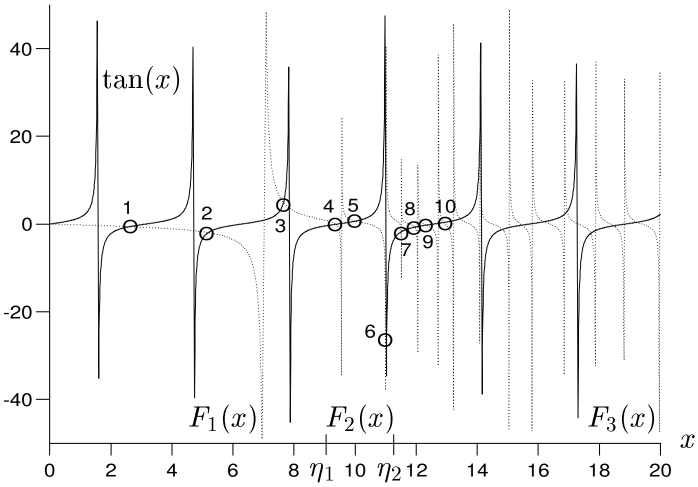

Figure 3: B_k^d - Functions tan, F_1, F_2 and F_3.

In I_1 we compare the three eigenvalues of B_k, B_k^d and B_k^n. With a precision $\varepsilon = 10^{-5}$, we get

m	$\gamma_m^n(k)+k^2\bar n_+^2$	$\gamma_m(k)+k^2\bar n_+^2$	$\gamma_m^d(k)+k^2\bar n_+^2$
1	$1,70593$	$1,70593$	$1,70593$
2	$6,72892$	$6,72892$	$6,72892$
3	$14,64787$	$14,64807$	$14,64835$

There is only a small difference for the third, the eigenvectors are also similar, see Figure 4. So, usually, $\gamma_1^d(k)$ and $\gamma_1^n(k)$ are good approximation of $\gamma_1(k)$. The approximation is not good if k is small or if h_1 and h_2 are near c. With $k=0.5$, $h_1=3$, $h_2=4$ we get one eigenvalue

m	$\gamma_m^n(k)+k^2\bar n_+^2$	$\gamma_m(k)+k^2\bar n_+^2$	$\gamma_m^d(k)+k^2\bar n_+^2$
1	$0,67664$	$0,69591$	$0,71770$

But, for $k = 0.5$, if we take $h_1 = h_2 = 100$ we get identical values

m	$\gamma_m^n(k) + k^2\bar{n}_+^2$	$\gamma_m(k) + k^2\bar{n}_+^2$	$\gamma_m^d(k) + k^2\bar{n}_+^2$
1	$0,69591$	$0,69591$	$0,69591$

With $k = 2$ but $h_1 = h_2 = 1.1$, very close to c, we have

m	$\gamma_m^n(k) + k^2\bar{n}_+^2$	$\gamma_m(k) + k^2\bar{n}_+^2$	$\gamma_m^d(k) + k^2\bar{n}_+^2$
1	$1,21853$	$1,70593$	$2,06836$
2	$5,12910$	$6,72892$	$8,27228$
3	$12,20251$	$14,64807$	$18,60825$

When $h_1 = h_2 = c$ we have an exact expression of $\gamma_m^n(k)$ and $\gamma_m^d(k)$:

$$\gamma_m^n(k) = -k^2\bar{n}_+^2 + \frac{(m-1)^2\pi^2}{4c^2}, \qquad \gamma_m^d(k) = -k^2\bar{n}_+^2 + \frac{m^2\pi^2}{4c^2}.$$

In I_2, with the data (11) and (12), we get three eigenvalues.

m	4	5	6
$\gamma_m^n(k)$	$-15,46142$	$-12,47721$	$-8,83024$
$\gamma_m^d(k)$	$-14,07743$	$-10,95298$	$-5,71381$

Finally, we give the first four eigenvalues in I_3.

m	7	8	9	10
$\gamma_m^n(k)$	$-3,75907$	$-2,48574$	$-1,10804$	$2,29668$
$\gamma_m^d(k)$	$-2,91438$	$-0,25858$	$1,98146$	$5,67769$

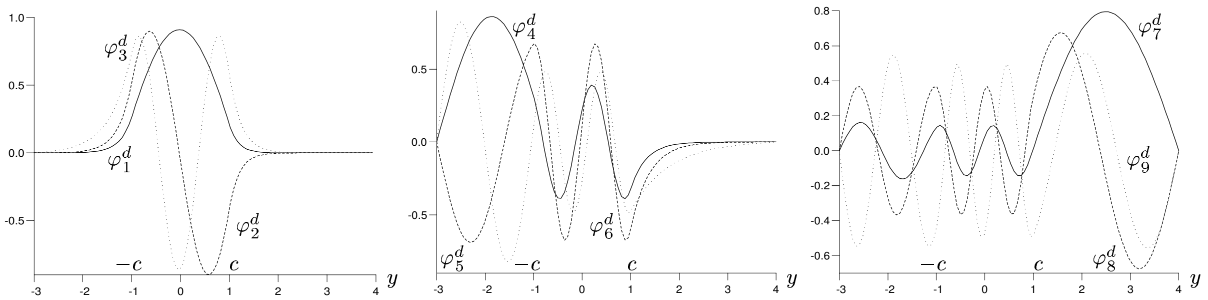

Figure 4: B_k^d - eigenvectors in I_1, I_2 and I_3.

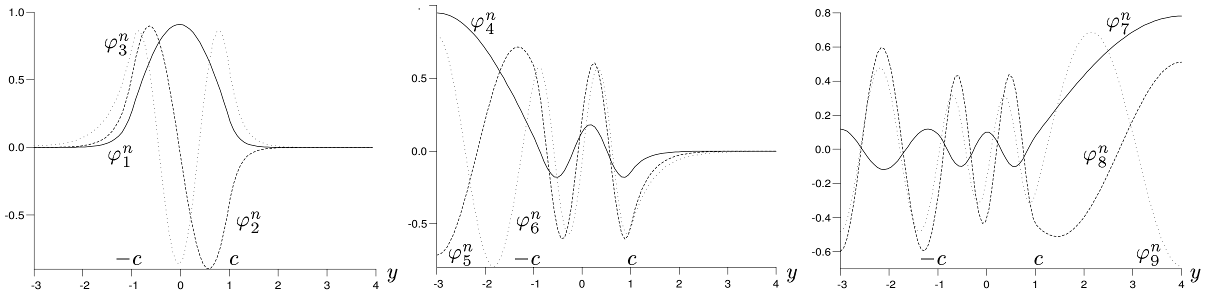

Figure 5: B_k^n - eigenvectors in I_1, I_2 and I_3.

3 The numerical method

We explain the method in three steps. First we write the problem in a bounded domain, then it is discretized with finite elements and finally we compute the eigenpairs for a matrix problem.

3.1 The problem in a bounded domain

We consider (P^d) and (P^n) as good approximations of (6) that we denote (P) ($\lambda_m(k)$ are the eigenvalues). Moreover, by (9), we see that when $\lambda_m^n(k) < \gamma_1(k)$, the difference $\lambda_m^d(k) - \lambda_m^n(k)$ give the precision of the approximation. We will see in the next subsection that some of the inequalities (9) hold also for the discretized problems.

Now, we write problems (P^{dl}) and (P^{nl}) stated in the bounded domain Ω_b and equivalent to (P^d) and (P^n). We use a series development of the solution in the exterior domain $\Omega_e = \Omega \backslash \Omega_b$ which is an exact representation of the solution on the vertical boundaries $\Sigma^\pm = \{\pm a\} \times [-d, d]$. It is the localized finite element method describe by Lenoir and Tounsi [10] in hydrodynamics, and then by Bonnet and Gmati [1, 7, 4] in guided optics when the medium is homogeneous or a diopter.

We describe the method for (P^{dl}), it is similar for (P^{nl}). We denote $\Gamma_b^\pm = [-a, a] \times \{\pm d\}$ the horizontal boundaries of Ω_b, $\Gamma_b = \Gamma_b^+ \cup \Gamma_b^-$, see Figure 6.

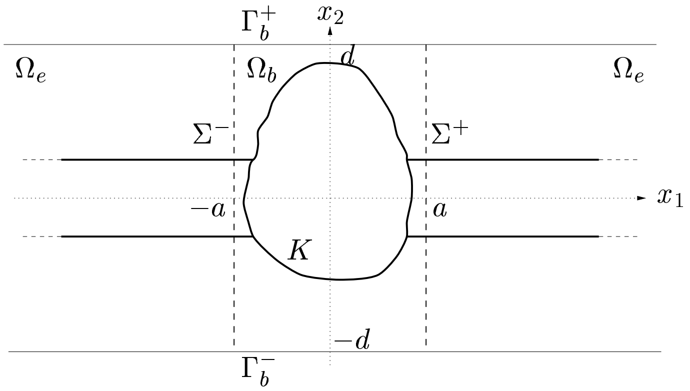

Figure 6: Bounded domain.

Let $I_d =]-d, d[$, $(\gamma_m^d(k), \varphi_m^d)$, $m \geq 1$, are the eigenpairs of the one-dimensional operator $B_k^d : H^2(I_d) \cap H_0^1(I_d) \longrightarrow L^2(I_d)$ defined by $B_k^d \varphi = \frac{d^2\varphi}{dx_2^2} - k^2\bar{n}^2\varphi$, see section 2. The set $(\varphi_m^d)_{m\geq1}$ is an orthonormal basis of $L^2(I_d)$. Let u the solution of (P^d) and $(x_1, x_2) \in \Omega_e$, we have

$$u(x_1, x_2) = \sum_{m\geq1} \alpha_m(x_1)\varphi_m^d(x_2),$$

and (5) give

$$\sum_{m\geq1} \left[-\frac{d^2\varphi_m^d}{dx_2^2}(x_2) - k^2\bar{n}^2\varphi_m^d(x_2) \right] \alpha_m(x_1) - \frac{d^2\alpha_m}{dx_1^2}(x_1)\varphi_m^d(x_2) = \lambda \sum_{m\geq1} \alpha_m(x_1)\varphi_m^d(x_2)$$

By the definition of φ_m^d we deduce

$$\sum_{m\geq1} \left[(\gamma_m^d(k) - \lambda)\alpha_m(x_1) - \frac{d^2\alpha_m}{dx_1^2}(x_1) \right] \varphi_m^d(x_2) = 0.$$

and thus

$$-\alpha_m''(x_1) = (\lambda - \gamma_m^d(k))\alpha_m(x_1).$$

If $\lambda - \gamma_m^d(k) > 0$ there is no solution in $L^2\left(]-\infty, -a[\cup]a, \infty[\right)$, and if $\lambda - \gamma_m^d(k) < 0$ we get

$$\begin{aligned}\alpha_m(x_1) &= C_m^+ e^{-\sqrt{-\lambda+\gamma_m^d(k)}\,x_1}, \quad \text{if } x_1 \geq a,\\ &= C_m^- e^{\sqrt{-\lambda+\gamma_m^d(k)}\,x_1}, \quad \text{if } x_1 \leq -a,\end{aligned}$$

where C_m^+ and C_m^- are constants to be determined. With $u_{|\Sigma^\pm} = \sum\limits_{m\geq 1} \alpha_m(\pm a)\varphi_m^d(x_2)$, we get

$$C_m^\pm = (u, \varphi_m^d)_{0,\Sigma^\pm}\, e^{\sqrt{-\lambda+\gamma_m^d(k)}\,a}.$$

We now have a development of u in each half exterior domain $\Omega_e^+ =]-d,d[\times]a,\infty[$ or $\Omega_e^- =]-d,d[\times]-\infty,-a[$ dependent on the value of u on Σ^+ or Σ^-:

$$u(x_1,x_2) = \sum_{m\geq 1} (u, \varphi_m^d)_{0,\Sigma^\pm}\, e^{\sqrt{-\lambda+\gamma_m^d(k)}\,(\mp x_1 + a)}\varphi_m^d(x_2) \quad \text{for } (x_1,x_2) \in \Omega_e^\pm. \tag{13}$$

This series expansion allows to define the problem

$$(P^{dl}) \qquad \begin{cases} \text{Find } u \in H^1(\Omega_b),\ u \neq 0,\ \lambda \in \mathbb{R} \text{ such that :} & \\ -\Delta u - k^2 n^2 u = \lambda u, & \text{in } \Omega_b,\\ u = 0, & \text{on } \Gamma_b,\\ \dfrac{\partial u}{\partial \nu}_{|\Sigma^\pm} = Q_\lambda^\pm u, & \text{on } \Sigma^\pm, \end{cases}$$

where ν is the unit external normal and

$$Q_\lambda^\pm u = \sum_{m\geq 1} \mp(u, \varphi_m^d)_{0,\Sigma^\pm} \sqrt{-\lambda + \gamma_m^d(k)}\ \varphi_m^d(x_2).$$

With the same method as described in [10] we prove that, for $\lambda < \gamma_1^d(k)$, the operator $Q_\lambda^\pm$ is continuous from $H^{\frac{1}{2}}(\Sigma^\pm)$ in $H^{-\frac{1}{2}}(\Sigma^\pm)$, with $\left\|Q_\lambda^\pm u\right\|^2_{-\frac{1}{2},\Sigma^\pm} = \|u\|^2_{\frac{1}{2},\Sigma^\pm}$ if $u \in H^{\frac{1}{2}}(\Sigma^\pm)$. The following proposition says how (P^{dl}) is equivalent to (P^d).

Proposition 2 *Let $\lambda < \gamma_1^d(k)$. If (u,λ) is solution of (P^d), then $(u_{|\Omega_b}, \lambda)$ is solution of (P^{dl}).*

Reciprocally, if $(\tilde{u},\lambda)$ is solution of (P^{dl}), then the function u defined by:

$$\begin{aligned} u &= \tilde{u} && \text{in } \Omega_b,\\ &= \sum_{m\geq 1} (\tilde{u}, \varphi_m^d)_{0,\Sigma^\pm}\, e^{\sqrt{-\lambda+\gamma_m^d(k)}\,(\mp x_1 + a)}\varphi_m^d(x_2) && \text{in} \Omega_e, \end{aligned}$$

is such that (u,λ) is solution of (P^d).

With the same steps we get that the problem (P^{nl}), obtained from (P^{dl}) in replacing $u = 0$ with $\frac{\partial u}{\partial \nu} = 0$ and $(\gamma_m^d(k), \varphi_m^d)$ with $(\gamma_m^n(k), \varphi_m^n)$, is equivalent to (P^n).

The condition on $\Sigma^{\pm}$ is non linear with respect to λ which is the value to compute. So we need to consider the solution as the invariant of a function. We define a sequence of problems (P_α^{dl}) for $\alpha \in]-k^2n_+^2, \gamma_1^d(k)[$:

$$(P_\alpha^{dl}) \qquad \begin{cases} \text{Find } u \in H^1(\Omega_b),\ u \neq 0,\ \lambda \in \mathbb{R} \text{ such that :} & \\ -\Delta u - k^2 n^2 u = \lambda u, & \text{in } \Omega_b, \\ u = 0, & \text{on } \Gamma_b, \\ \dfrac{\partial u}{\partial \nu}_{|\Sigma^{\pm}} = Q_\alpha^{\pm} u, & \text{on } \Sigma^{\pm}, \end{cases}$$

of which the variational form is

$$\begin{cases} \text{Find } u \in V,\ u \neq 0,\ \lambda(\alpha) \in \mathbb{R} \text{ such that :} \\ a_\alpha(u,v) = \lambda(\alpha)(u,v)_{0,\Omega_b}, \quad \forall v \in V, \end{cases}$$

where $V = \{u \in H^1(\Omega_b) / \, u = 0 \text{ on } \Gamma_b\}$ and

$$\begin{aligned} a_\alpha(u,v) = (\nabla u, \nabla v)_{0,\Omega_b} &- k^2 (n^2 u, v)_{0,\Omega_b} \\ &+ \sum_{m\geq 1} \sqrt{-\alpha + \gamma_m^d(k)}\,(u,\varphi_m^d)_{0,\Sigma^+} (\varphi_m^d, v)_{0,\Sigma^+} \\ &+ \sum_{m\geq 1} -\sqrt{-\alpha + \gamma_m^d(k)}\,(u,\varphi_m^d)_{0,\Sigma^-} (\varphi_m^d, v)_{0,\Sigma^-}. \end{aligned}$$

Then, $(\lambda_m^{dl}(\alpha,k), u_{m,\alpha}^{dl})$ is solution of (P^d) if and only if

$$\lambda_m^{dl}(\alpha,k) = \alpha. \tag{14}$$

Proposition 3 *let a fixed α, the bilinear form a_α is continuous on V. Moreover, $\forall u \in V$:*

$$a_\alpha(u,u) \geq \|\nabla u\|_{0,\Omega_b}^2 - k^2 n_+^2 \|u\|_{0,\Omega_b}^2.$$

Consequently, the solutions of (P_α^{dl}), denoted $(u_{m,\alpha}^{dl}, \lambda_m^{dl}(\alpha,k))$, are a countable sequence such that $\lambda_m^{dl}(\alpha,k)$ tends to ∞ with m, and the values $\lambda_m^{dl}(\alpha,k)$ are characterized by

$$\lambda_m^{dl}(\alpha,k) = \inf_{H_m \in \mathscr{H}_m(V)} \sup_{\substack{u \in H_m \\ u \neq 0}} \frac{a_\alpha(u,u)}{\|u\|_{0,\Omega_b}^2}, \quad m \geq 1. \tag{15}$$

We deduce from the formulas (15) that the functions $\alpha \longmapsto \lambda_m^{dl}(\alpha,k)$ are descending, they are also continuous, see [5]. Consequently the equation (14) has at most one solution.

3.2 Discretization

We use $\mathbb{P}_1$ Lagrange finite-elements to discretize all the previous problems. We show this for (P_α^{dl}). Let T_h be a triangulation of Ω_b such that $\bar{\Omega}_b = \cup_{\tau \in T_h} \tau$, $V_h = \{v_h \in C^0(\bar{\Omega}_b) \,/\, v_{h|\tau} \in \mathbb{P}_1,\ \forall \tau \in T_h\}$ and

$$V_h^0 = \{v_h \in V_h \,/\, v_h = 0 \text{ sur } \Gamma_b\}.$$

Then, we need to cut the series expansion of the boundary condition on Σ, retaining only a finite number M of terms, and the discretized problem $(P_{\alpha,h}^{dl})$ is:

$$(P_{\alpha,h}^{D,L}) \qquad \begin{cases} \text{Find } u \in V_h^0,\ u \neq 0,\ \lambda \in \mathbb{R} \text{ such that :} \\ \tilde{a}_\alpha(u, v_h) = \lambda(u, v_h)_{0,\Omega_b}, \quad \forall v_h \in V_h^0, \end{cases}$$

with
$$\begin{aligned}\tilde a_\alpha(u,v) = (\nabla u,\nabla v)_{0,\Omega_b} &\quad - k^2(u,v)_{0,\Omega_b}\\ &\quad + \sum_{m=1}^{M}\sqrt{-\alpha+\gamma_m^d(k)}\,(u,\varphi_m^d)_{0,\Sigma^+}(\varphi_m^d,v)_{0,\Sigma^+}.\\ &\quad + \sum_{m=1}^{M} -\sqrt{-\alpha+\gamma_m^d(k)}\,(u,\varphi_m^d)_{0,\Sigma^-}(\varphi_m^d,v)_{0,\Sigma^-}.\end{aligned}$$

For an eigenvalue problem, the convergence of the localized finite element method is studied in [4]: it is proved that the error decreases faster than any power of $\frac{1}{M}$.

We denote by N_h the number of degrees of freedom (values of the function at the points of the triangulation except these on the boundary Γ_b) of V_h^0, $w_i,\ i=1,\dots,N_h$, the usual basis functions of V_h^0 and U_i the value of u at the i^{th} point of the triangulation. Then we have

$$u = \sum_{i=1}^{N_h} U_i w_i$$

and $(P_{\alpha,h}^{dl})$ is a linear system

$$[A(\alpha)]\,U_\alpha = \lambda(\alpha,k)[M]\,U_\alpha,$$

where $U_\alpha = (U_i)_{1\le i\le N_h}$, $[A(\alpha)] = [R] + [\tilde M] + [L(\alpha)]$, for $1\le i,j\le N_h$:

$$R_{ij} = \int_\Omega \nabla w_i.\nabla w_j\,dx,\quad \tilde M_{ij} = -k^2\int_\Omega n^2 w_i.w_j\,dx,\quad M_{ij} = \int_\Omega w_i.w_j\,dx$$

and

$$L_{ij} = \sum_{m=1}^{M}\sqrt{-\alpha+\gamma_m^d(k)}\,(w_i,\varphi_m^d)_{0,\Sigma^\pm}(\varphi_m^d(x_2),w_j)_{0,\Sigma^\pm}.$$

If i or j is the number of a point not on Σ then $L_{ij}=0$. If the points on Σ are numbered from 1 to N_Σ, the matrix $[L(\alpha)]$ is a full block $(L_{ij})_{1\le i,j\le N_\Sigma}$. It is because the condition on $\Sigma^\pm$ is non local.

The problem $(P_{\alpha,h}^{dl})$ has N_h real eigenvalues, denoted $\lambda_{m,h}^{dl}(\alpha,k)$ and characterized by:

$$\lambda_{m,h}^{dl}(\alpha,k) = \inf_{H_m\in\mathscr{H}_m(V_h^0)}\ \sup_{\substack{u\in H_m\\ u\neq 0}} \frac{\tilde a_\alpha(u,u)}{\|u\|_{0,\Omega_b}^2},\quad m\ge 1.$$

Proposition 4 *The functions $\alpha\longmapsto\lambda_{m,h}^{dl}(\alpha,k)$ are continuous and decreasing on $]-k^2n_+^2,\gamma_1^d(k)[$.*

When it exists, the fix point
$$\alpha = \lambda_{m,h}^{dl}(\alpha,k) \tag{16}$$
is solution of the discretized problem (P_h^{dl}):

$$(P_h^{dl})\qquad \begin{cases}\text{Find } u\in V_h^0,\ u\neq 0,\ \alpha\in\mathbb{R} \text{ such that:}\\ \tilde a_\alpha(u,v_h) = \alpha(u,v_h)_{0,\Omega_b},\quad \forall v_h\in V_h^0.\end{cases}$$

We denote it $\lambda_{m,h}^{dl}(k)$.

In the same way, we discretize the problems (P_α^{nl}) and (P^{nl}), (P^{dd}) and (P^{nn}).

From the min-max formulae we can deduce the following inequalities for a triangulation T_h and M big enough:

$$\lambda_m(k)\le\lambda_m^d(k)\le\lambda_{m,h}^{dl}(k).$$

Moreover, if T_{h_2} is a triangulation included in another triangulation T_{h_1} (it means that each summit of T_{h_1} is a summit of T_{h_2} and each triangle of T_{h_2} is included in a triangle of T_{h_1}), we have

$$\lambda_m^d(k) \leq \lambda_{m,h_2}^{dl}(k) \leq \lambda_{m,h_1}^{dl}(k).$$

Same kind of inequalities hold for the other problems:

$$\lambda_m^{dd}(k) \leq \lambda_{m,h_2}^{dd}(k) \leq \lambda_{m,h_1}^{dd}(k); \quad \lambda_m^{nn}(k) \leq \lambda_{m,h_2}^{nn}(k) \leq \lambda_{m,h_1}^{nn}(k); \quad \lambda_m^{n}(k) \leq \lambda_{m,h_2}^{nl}(k) \leq \lambda_{m,h_1}^{nl}(k).$$

Since we have (9), for a triangulation accurate enough we will have

$$\min(\lambda_{m,h}^{nn}(k), \gamma_1(k)) \leq \min(\lambda_{m,h}^{nl}(k), \gamma_1(k)) \leq \lambda_m(k) \leq \lambda_{m,h}^{dl}(k) \leq \lambda_{m,h}^{dd}(k).$$

Remark 1 *When the eigenpair $(\lambda_{m,h}^{dl}(k), u_{m,h}^{dl})$ is computed, $u_{|\Sigma}$ is known and (13) allows to compute the eigenfunction in Ω_e.*

3.3 Computing

To compute the eigenpairs we use the inverse power method with shift, see [18], which yields the eigenvalue closest to shift θ. We consider the linear system $[A(\alpha) - \theta M]U = \mu[M]U$ instead of $[A(\alpha)]U = \lambda[M]U$, and the inverse power method give the smallest value μ. Then $\lambda = \theta + \mu$ is the eigenvalue closest to θ.

The eigenvalues are in the interval $]-k^2n_+^2, \gamma_1(k)[$. Thus to compute the first one we choose $\theta = -k^2n_+^2$, and for the others a θ in the previous interval. Moreover, with this shift we have adimensional quantities $\lambda_m(k) + k^2n_+^2$ which satisfy $0 \leq \lambda_m(k) + k^2n_+^2 \leq \gamma_1(k) + k^2n_+^2 < \frac{\pi^2}{h^2}$ whereas $\lambda_m(k)$ tends to $-\infty$ as k tends to infinity.

The other question is to solve (16). We search $\alpha \in]-k^2n_+^2, \gamma_1(k)[$ such that $\alpha = g(\alpha)$ where $g(\alpha) = \lambda_{m,h}^{dl}(\alpha, k)$. The function g is decreasing and continuous, we have $g(-k^2n_+^2) \geq -k^2n_+^2$ (because $\tilde{a}_\alpha(u,u) \geq -k^2n_+^2\|u\|_{0,\Omega_b}^2$), then (16) has a solution if and only if

$$g(\gamma_1(k)) < \gamma_1(k). \tag{17}$$

If (17) is satisfied we take $\alpha_0 = -k^2n_+^2$ as initial value and the iterative process is defined by

$$\alpha_{s+1} = \frac{\gamma_1(k) \cdot \dfrac{g(\alpha_s) - g(\gamma_1(k))}{\alpha_s - \gamma_1(k)} - g(\gamma_1(k))}{\dfrac{g(\alpha_s) - g(\gamma_1(k))}{\alpha_s - \gamma_1(k)} - 1}, \tag{18}$$

the convergence criterion being $|\alpha_{s+1} - \alpha_s| < \varepsilon$, where ε is the wanted accuracy.

We can now give the general algorithm where we take $\gamma_1^d(k)$ as a good approximation of $\gamma_1(k)$.

• Data: k, $n(x)$, mesh of Ω_b, M, ε, θ.

• Step 1: computing of $(\gamma_m^d(k), \varphi_m^d)$ for $m = 1, \cdots, M$, of the elementary finite element matrix, and assembling of the matrix independent of α: $[C] = [R] + [\tilde{M}] + \theta[M]$.

• Step 2: Existence test: $g(\gamma_1^d(k)) < \gamma_1^d(k)$.
  ▷ $\alpha = \gamma_1^d(k)$.
  ▷ Assignment of the terms $\sqrt{-\alpha + \gamma_m^d(k)}$.
  ▷ Assembling of the matrix $[L(\alpha)]$ and $[A(\alpha)] = [C] + [L(\alpha)]$.

▷ Computing of $g(\gamma_1^d(k))$ by the inverse power method.
▷ If $g(\gamma_1^d(k)) \geq \gamma_1^d(k)$ then STOP.

- Step 3: $\alpha_0 = -k^2 n_+^2$ and computing of $g(\alpha_0)$ like in the step 2.
- Step 4: Iterations.
  ▷ Computation of α_{s+1} by (18).
  ▷ Convergence test:
    ∘ if $|\alpha_{s+1} - \alpha_s| < \varepsilon$ then $\lambda = \alpha_{s+1}$ is the solution.
    ∘ else: $\alpha_s := \alpha_{s+1}$ and Computing of $g(\alpha_s)$ like in the step 2.

Remark 2 *In the iterative process, α is modified, but to compute the matrix $[L(\alpha)]$ (and $[A(\alpha)]$) we need only to change coefficients $\sqrt{-\alpha + \gamma_m^d(k)}$ and assemble another time the matrix, because the elementary matrix $[E] = (E_{im})_{\substack{1\le i\le N_\Sigma \\ 1\le m\le M}}$, such that $E_{im} = (w_i, \varphi_m^d)_{L^2(\Sigma)}$, is preserved and then*

$$L_{ij} = \sum_{m=1}^{M} \sqrt{-\alpha + \gamma_m^d(k)}\, E_{im} E_{mj}.$$

It is important to remark, for the sake of accuracy, that the integrals giving E_{im} are computed with exact formulas.

In the examples we have chosen, the domain is symmetrical and we compute only on a half domain with only one boundary, Σ^+, with a localized finite element condition.

For the implementation of this numerical method we have used and developed the finite element code MÉLINA, see [12]. The computing is done in single precision with a SUN-Ultra1. The visualization of the results is done with GRAME developed by Pascal Gentil from University Rennes 1, for the result files of MÉLINA.

4 Numerical results

In the first subsection we give numerical tests of the efficiency of the method and in the second subsection we present cases where the exact condition on the vertical boundaries is essential.

Here we give results for functions $\bar{n}(x_2)$ taking only 3 values, we have (1) and $\bar{n}(\xi) = \bar{n}_+$ for $|\xi| \leq c$, where $\bar{n}_+ = \|\bar{n}\|_{\infty,\mathbb{R}} > n_b$. Moreover we are going to consider the function $n(x)$ described on Figure 7, and we will give values to the parameters h_a, h_b, H, a, l, L, n_b, n_+, n_t (the unit for the distances is the micrometer).

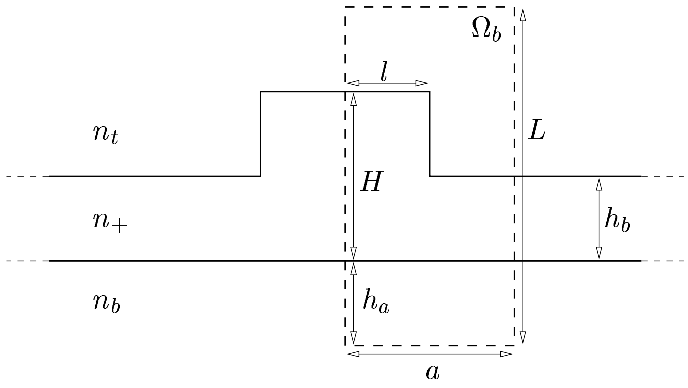

Figure 7: Rib waveguide.

We denote $\mu^{dl}_{m,h}(k)$ the adimensional quantities $\lambda^{dl}_{m,h}(k)+k^2n_+^2$, and by analogy we have $\mu^{dd}_{m,h}(k)$, $\mu^{nl}_{m,h}(k)$ and $\mu^{nn}_{m,h}(k)$. The computed eigenvectors U are such that $|U_i|\leq 1$ and $\max_i |U_i| = 1$. They are presented with isovalues which are 0 on the horizontal boundaries and ±1 at the center.

4.1 Tests

There is a difficulty to find the good test because to compare with an exact solution we need a simpler problem where the dependence with respect to x_2 of the solution is only one of the spectral functions φ^d_m, see paragraph 4.1.1. To have a dependence with respect to x_2 different from the functions φ^d_m, we get a problem without an exact solution. But we can compare the results between the problem stated in a big and a small set, the second included in the first, see paragraph 4.1.2. In the paragraph 4.1.3 we present convergence studies with respect to M and h the mesh size.

Comparing two vectors U and W with the same dimension N, we consider two kind of errors, the quadratic error E_q and the relative quadratic error E_r:

$$E_q(U,W) = \left(\frac{1}{N}\sum_{i=1}^N (U_i - W_i)^2\right)^{\frac12}; \qquad E_r(U,W) = \frac{2\left(\sum_{i=1}^N (U_i-W_i)^2\right)^{\frac12}}{\left(\sum_{i=1}^N U_i^2\right)^{\frac12} + \left(\sum_{i=1}^N W_i^2\right)^{\frac12}}.$$

4.1.1 With an exact solution

The domain is $\Omega = \mathbb{R}_*^+ \times]0,d[= \Omega_b \cup \Omega_e$ with $\Omega_b =]0,a[\times]0,d[$. We denote by z and y the space variables. The boundaries of Ω are $\Gamma_1(z=0)$, $\Gamma_2(y=0)$, $\Gamma_3(y=d)$. Let $\Sigma = \{a\}\times]0,d[$.

We denote by p a non negative integer parameter. The solution of the problem

$$\begin{cases} \text{Find } u \in H^1(\Omega), \text{ such that :} \\ \triangle u = 0, & \text{in } \Omega, \\ u = 0, & \text{on } \Gamma_1, \\ \dfrac{\partial u}{\partial \nu} = g, & \text{on } \Gamma_2 \cup \Gamma_3, \end{cases}$$

where

$$g(y) = \frac{p\pi}{d}\sin\left(\frac{p\pi}{d}y\right),$$

is

$$u(z,y) = e^{-\frac{p\pi}{d}z}\sin\left(\frac{p\pi}{d}y\right).$$

The solutions (γ_m, φ_m) of the one-dimensional problem

$$\begin{cases} \text{Find } \varphi \in H^1_0(]0,d[),\ \varphi \neq 0,\ \gamma\in\mathbb{R} \text{ such that :} \\ -\varphi''(y) = \gamma\,\varphi(y), \end{cases}$$

are, for $m \geq 1$,

$$\gamma_m = \frac{m^2\pi^2}{d^2} \quad \text{and} \quad \varphi_m(y) = \sqrt{\frac{2}{d}}\sin\left(\frac{m\pi}{d}y\right).$$

The localized finite element method leads to the variational problem

$$\begin{cases} \text{Find } u \in V, \text{ such that :} \\ (\nabla u, \nabla v)_{0,\Omega_i} + \displaystyle\sum_{m\geq1}(u,\varphi_m)_{0,\Sigma}\frac{m\pi}{d}\varphi_m(y)(\varphi_m, v)_{0,\Sigma} = (g,v)_{0,\Gamma_1},\ \forall v\in V, \end{cases}$$

where $V = \{v \in H^1(\Omega_b) \,/\, v(z,0) = v(z,d) = 0,\ \forall z \in [0,a]\}$.

As previously, we denote M the order of the truncature of the series and we discretize the problem. There is only one non trivial term in the series because

$$(u, \varphi_p)_{0,\Sigma} = \sqrt{\frac{d}{2}}\, e^{-\frac{m\pi}{d}a} \quad \text{and} \quad (u, \varphi_m)_{0,\Sigma} = 0 \ \text{ if } m \neq p.$$

It's why we get bad results if $M < p$ and good ones if $M \geq p$.

We choose $d = \pi$, $c = 1$ and a mesh with 816 triangles and 451 nodes. We note U_{ex} the exact solution and U the computed vector. We give $E_r(U, U_{ex})$ in the following table, depending on M and p.

$p \backslash M$	1	2	3	7
1	0.131%	0.132%	0.132%	0.132%
2	13.552%	0.632%	0.632%	0.631%
3	4.796%	4.796%	1.455%	1.455%

The eigenvector U has p oscillations, then, with a same mesh, the accuracy of the finite element approximation decreases as p increases.

4.1.2 With a smaller set included in a bigger

We consider the function $n(x)$ as on the Figure 7 with $n_+ = 3.44$, $n_b = 3.435$, $n_t = 1$, $h_b = 3.5$, $H = 6$, $l = 2$, $h_a = 5$, $L = 11.5$. Let two values for a, $a_1 = 3$ and $a_2 = 10$, associated with two sets $\Omega_1 \subset \Omega_2$. With $k = 4$ we compute the first eigenpair of (P_h^{dl}) for the two domains, denoted $(\lambda_{\Omega_1}, U_{\Omega_1})$ and $(\lambda_{\Omega_2}, U_{\Omega_2})$. We can measure the efficiency of the method in comparing the results. The meshes of Ω_1 (932 triangles and 511 nodes) and Ω_2 (2158 triangles and 1166 nodes) are the same on Ω_1, see Figure 8.

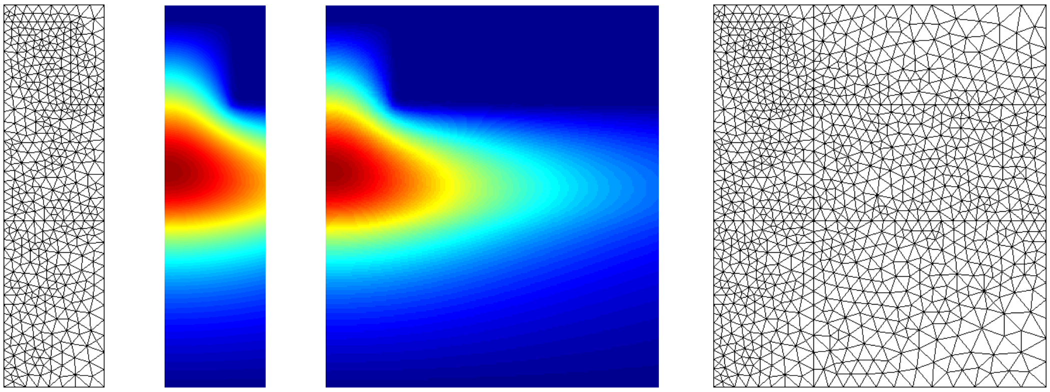

Figure 8: Mesh and first eigenvector of Ω_1 and Ω_2.

With $M = 7$, we get for the eigenvalue

$$|\lambda_{\Omega_1} - \lambda_{\Omega_2}| = 1.397 \times 10^{-3}, \qquad \frac{|\lambda_{\Omega_1} - \lambda_{\Omega_2}|}{\frac{1}{2}(\lambda_{\Omega_1} + \lambda_{\Omega_2})} = 0.400\%,$$

and for the eigenvectors, see Figure 8

$$E_q(U_{\Omega_1}, U_{\Omega_2}) = 1.460 \times 10^{-3}, \qquad E_r(U_{\Omega_1}, U_{\Omega_2}) = 0.308\%.$$

If we plot $E_q(U_{\Omega_1}, U_{\Omega_2})$ against M, Figure 9, we see that for $M > 7$ the error remains unchanged.

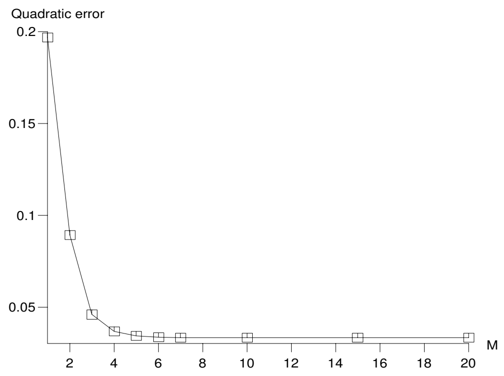

Figure 9: Quadratic error against M.

4.1.3 Convergence

Again, we consider a function $n(x)$ as on the Figure 7 with $n_+ = 3$, $n_b = 2$, $n_t = 1$, $h_b = 0.4$, $H = 0.6$, $l = 0.2$, $h_a = 0.4$, $L = 1$ and $a = 0.4$. We set $k = 10$. We build a sequence of 5 meshes with a step h smaller and smaller. We call them mesh$p$ with $p = 2, 4, 8, 16, 32$, see Figure 10. We obtain Mesh$2p$ from Mesh$p$ in dividing each triangle in 4, adding 3 nodes, the mid-point of each edge. Then the step of mesh$p$ is $h = h_0/p$ where $h_0 = \frac{2\sqrt{2}}{5}$.

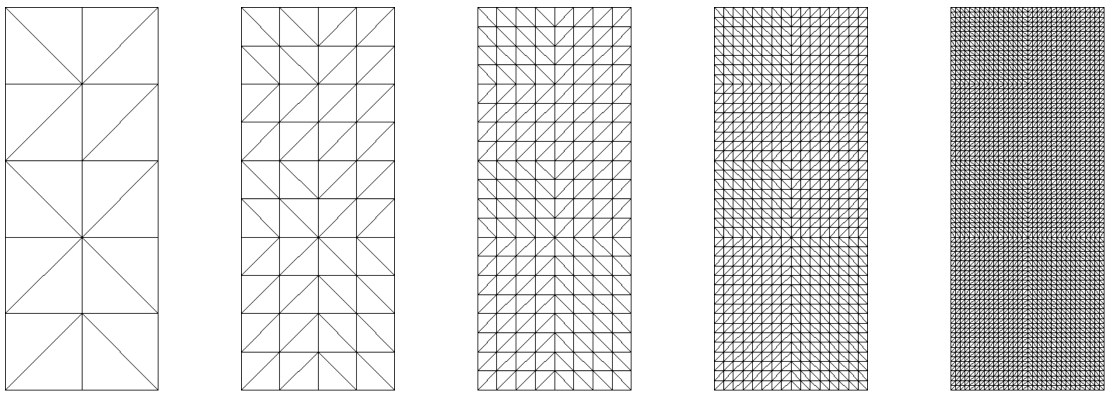

Figure 10: Meshes for convergence study: $p = 2,\ 4,\ 8,\ 16,\ 32$.

Firstly we are going to study the finite element convergence for the 4 different problems: (P_h^{nn}), (P_h^{nl}), (P_h^{dl}) and (P_h^{dd}). We give for $M = 7$ the first computed eigenvalue of these problems, with finite elements P_1 in the first table and P_2 in the second.

$\mu\backslash p$	2	4	8	16	32
$\mu_{1,h}^{nn}$	45.1437035	37.9420433	35.5640564	34.8692017	34.6836395
$\mu_{1,h}^{nl}$	-	40.0518761	38.1926460	37.6196823	37.4647102
$\mu_{1,h}^{dl}$	-	40.0533180	38.1955109	37.6232567	37.4684792
$\mu_{1,h}^{dd}$	58.9479027	48.4830246	45.4838829	44.6389236	44.4158134

First eigenvalue computed with P_1 finite-elements

$\mu\backslash p$	2	4	8	16	32
$\mu^{nn}_{1,h}$	35.7251358	34.7970390	34.6387024	34.6213951	34.6197395
$\mu^{nl}_{1,h}$	38.3762856	37.5653000	37.4276657	37.4125214	37.4112396
$\mu^{dl}_{1,h}$	38.4295959	37.5696564	37.4315186	37.4163399	37.4150276
$\mu^{dd}_{1,h}$	45.9496460	44.5531921	44.3614311	44.3414268	44.3396988

First eigenvalue computed with P_2 finite-elements

In the first table for $p = 2$ there isn't a value for (P_h^{nl}) and (P_h^{dl}) because the mesh is not accurate enough, the eigenvalue is increased too much and the existence test is not satisfied $(g(\gamma_1(k)) > \gamma_1(k))$. We can see that for each mesh we have $\mu^{nn}_{1,h} \leq \mu^{nl}_{1,h} \leq \mu^{dl}_{1,h} \leq \mu^{dd}_{1,h}$, for each problem $\mu_{1,h_p} \geq \mu_{1,h_{2p}}$, and the difference $\left|\mu^{nn}_{1,h} - \mu^{dd}_{1,h}\right| \simeq 10$ stay big while $\left|\mu^{nl}_{1,h} - \mu^{dl}_{1,h}\right| \simeq 4 \times 10^{-3}$ is small. Indeed, for k great enough the condition on the horizontal boundaries is not important, but in the boundary Σ it is. In the Figure 11 we see the differences between the eigenvectors: as for the eigenvalue, there is a big difference not between (P_h^{nl}) and (P_h^{dl}) but with the others.

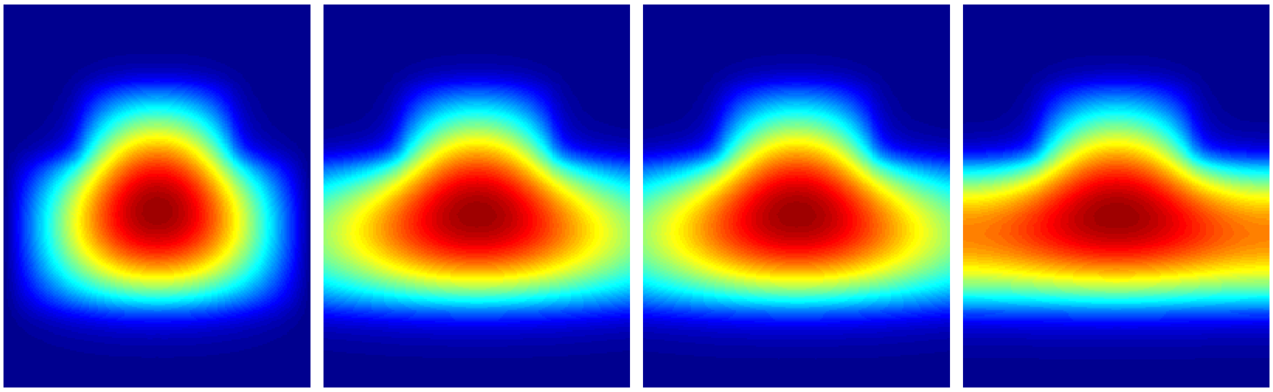

Figure 11: Symmetrized eigenvectors: $U^{dd}_{1,h}$, $U^{dl}_{1,h}$, $U^{nl}_{1,h}$, $U^{nn}_{1,h}$ - mesh16.

If we took the solution P_2 with $p = 32$ as an exact solution, we get, with the first table, the P_1 finite element convergence h^2, see Figure 12.

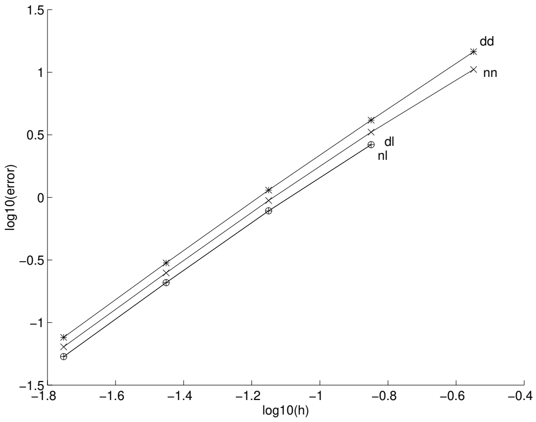

Figure 12: Convergence curves P_1 for the 4 problems.

Secondly, we study the dependence with respect to M. For M from 1 to 9, we give in the following tables $\mu^{dl}_{1,h}$ computed with P_1 and P_2 finite-elements.

$p\backslash M$	1	2	3	4	5	6	7	8	9
2	-	-	-	-	-	-	-	-	-
4	40.0480	40.0513	40.0523	40.0523	40.0528	40.0532	40.0533	40.0561	40.0562
8	38.1891	38.1948	38.1953	38.1954	38.1955	38.1955	38.1955	38.1957	38.1957
16	37.6164	37.6229	37.6232	37.6232	37.6232	37.6232	37.6233	37.6232	37.6233
32	37.4614	37.4682	37.4684	37.4684	37.4685	37.4685	37.4685	37.4685	37.4685

$\mu^{dl}_{1,h}$ - P_1 Finite-elements.

$p\backslash M$	1	2	3	4	5	6	7	8	9
2	38.4088	38.4153	38.4169	38.4181	38.4227	38.4287	38.4296	38.4325	38.4384
4	37.5627	37.5693	37.5696	37.5696	37.5696	37.5697	37.5697	37.5697	37.5697
8	37.4245	37.4313	37.4315	37.4315	37.4316	37.4315	37.4315	37.4315	37.4315
16	37.4093	37.4161	37.4164	37.4164	37.4164	37.4164	37.4163	37.4164	37.4164
32	37.4079	37.4148	37.4151	37.4151	37.4150	37.4149	37.4151	37.4150	37.4150

$\mu^{dl}_{1,h}$ - P_2 Finite-elements.

We can see in these tables that, for a mesh accurate enough, the five first terms of the series only are important.

4.2 Results

We have proved in [3] that when k increases, the eigenvector is more and more confined in the area where $n(x) = n_+$. When $\bar{n}_+ < n_+$ this area is bounded and the results are the same than with a constant function $\bar{n}(x_2)$ and an homogeneous Dirichlet conditions is adequate on all the boundaries, see paragraph 4.2.1. But when $\bar{n}_+ = n_+$, the eigenvector can be less and less confined horizontally and the exact condition is useful, see paragraphs 4.2.2 and 4.2.3.

4.2.1 Example 1

Let the function $n(x)$ as on the Figure 13 with $n_+ = 3.44$, $\bar{n}_+ = 3.38$, $n_b = 3.17$, $n_t = 1$, $h_b = 1$, $H = 1.5$, $l = 1$, $h_a = 1.5$, $L = 3.2$ and $a = 2$. The mesh has 981 triangles and 524 nodes. We give on the Figure 14 the representation of the functions $k \longmapsto \mu^{dl}_{m,h}(k)$ for $m = 1, 2, 3$, and on the Figure 15 the three associated eigenvectors for $k = 10$. When k is big enough, the stratified medium doesn't play an important role and the exact condition on Σ is not useful.

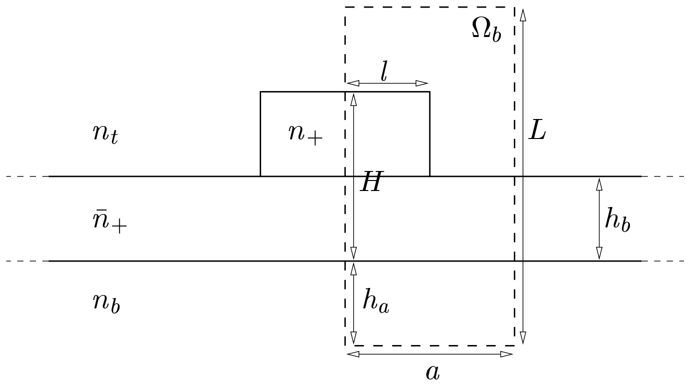

Figure 13: Example 1 - $n(x)$.

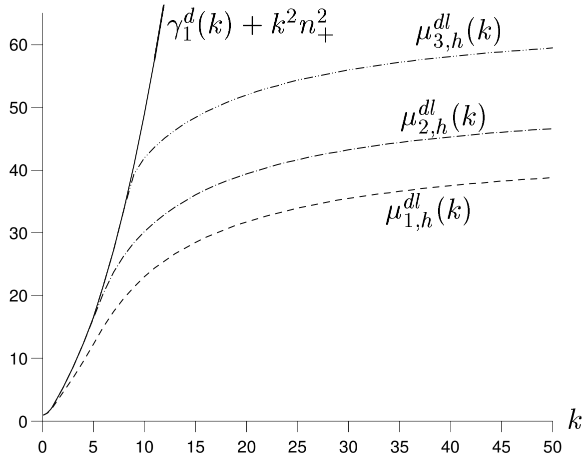

Figure 14: Example 1 - Functions $k \longmapsto \mu_{m,h}^{dl}(k)$ for $m = 1, 2, 3$.

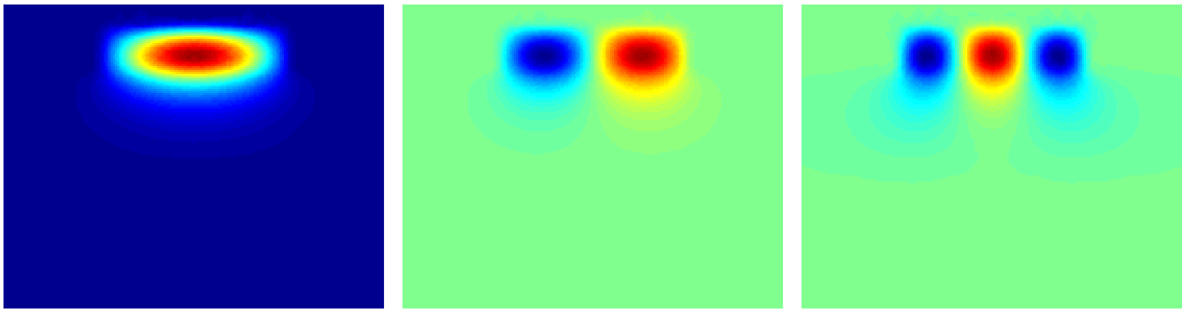

Figure 15: Example 1 - Symmetrized eigenvectors: $U_{1,h}^{dl}$, $U_{2,h}^{dl}$, $U_{3,h}^{dl}$ - $k = 10$.

4.2.2 Example 2

Let $n(x)$ the same function and the same mesh than in the previous paragraph in replacing $n_+ = 3.44$ with $n_* = 3.38$ and $\bar{n}_+ = 3.38$ with $n_+ = 3.44$, see Figure 13. So, we have $n_+ = \bar{n}_+$ and an unbounded area where $n(x) = n_+$. Theoretically, see [3], the first eigenpair exists for each $k > 0$ with an eigenvector which is less and less confined horizontally but more and more vertically as k increases. Numerically we find back this result: when k increases, the eigenvector concentrates vertically but not horizontally. In fact it concentrates horizontally up to about $k = 5$, when $\left|\lambda_{1,h}^{dl}(k) - \gamma_1^d(k)\right|$ is maximum, and then extends more and more, see Figure 16 and 17. Here, the exact condition on Σ is essential.

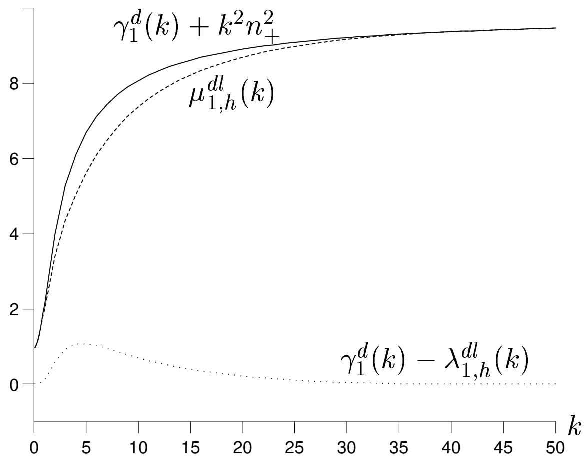

Figure 16: Example 2 - Function $k \longmapsto \mu_{1,h}^{dl}(k)$.

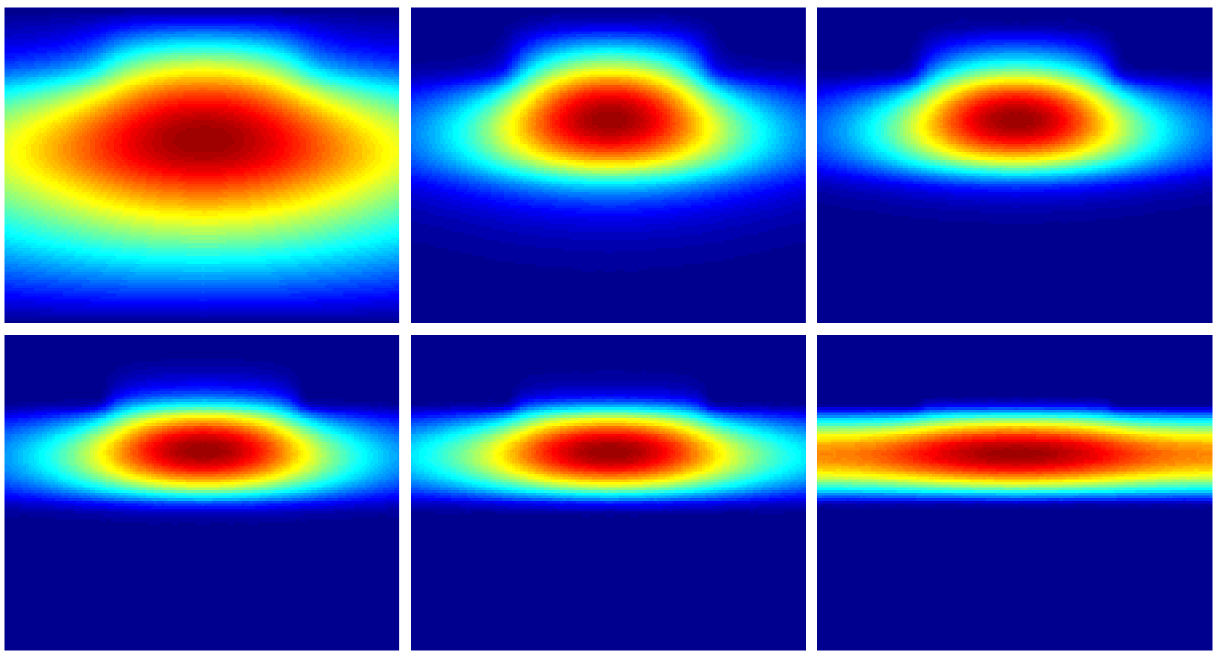

Figure 17: Example 2 - First symmetrized eigenvector for $k = 1, 3, 5, 10, 15, 40$.

4.2.3 Example 3

We consider the function $n(x)$ as on the Figure 18 with $n_+ = 3.44$, $n_* = 3.38$, $n_b = 3.17$, $n_t = 1$, $h_b = 1$, $H = 2$, $l = 1.5$, $l_* = 0.5$, $h_* = 0.5$, $h_a = 1.5$, $L = 3.7$ and $a = 2$. It is a case where the first eigenvector exists for $0 < k < k_*$ and disappears for $k > k_*$, see [3]. Numerically, we see that the eigenvector is more and more confined in both directions up to about $k = 2.5$, then it splits in two parts and expands horizontally before it vanishes for $k > 9$, see Figure 19 and 20. In this example, the exact condition on Σ is also useful.

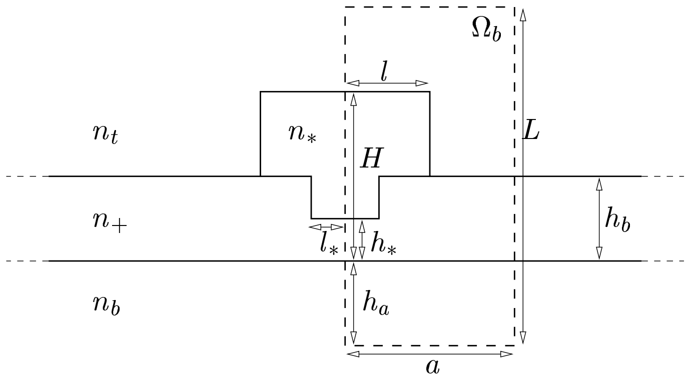

Figure 18: Example 3 - $n(x)$.

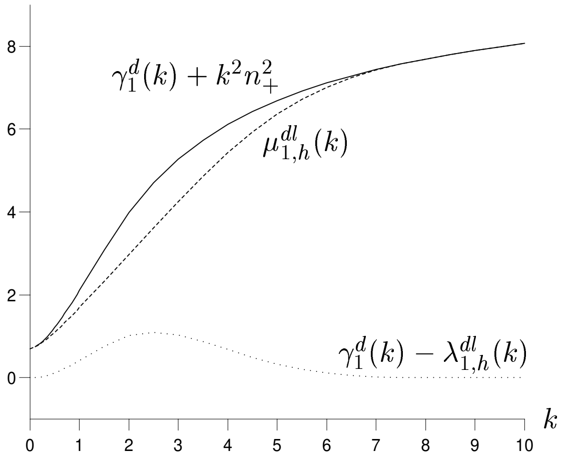

Figure 19: Example 3 - Function $k \longmapsto \mu_{1,h}^{dl}(k)$.

Conclusion

With the proposed method, we are able to study phenomena which are not well confined laterally like in the examples 2 and 3 of subsection 4.2. The lateral boundary condition allows to put the boundary close to the core of the structure and, after computation, (13) give the solution in all the lateral exterior domain.

Moreover, the difference between the solutions of (P_h^{dl}) and (P_h^{nl}) gives an estimate of the error coming from the lower and upper boundary conditions. This difference is small because the energy is well confined in the central layer of the guide.

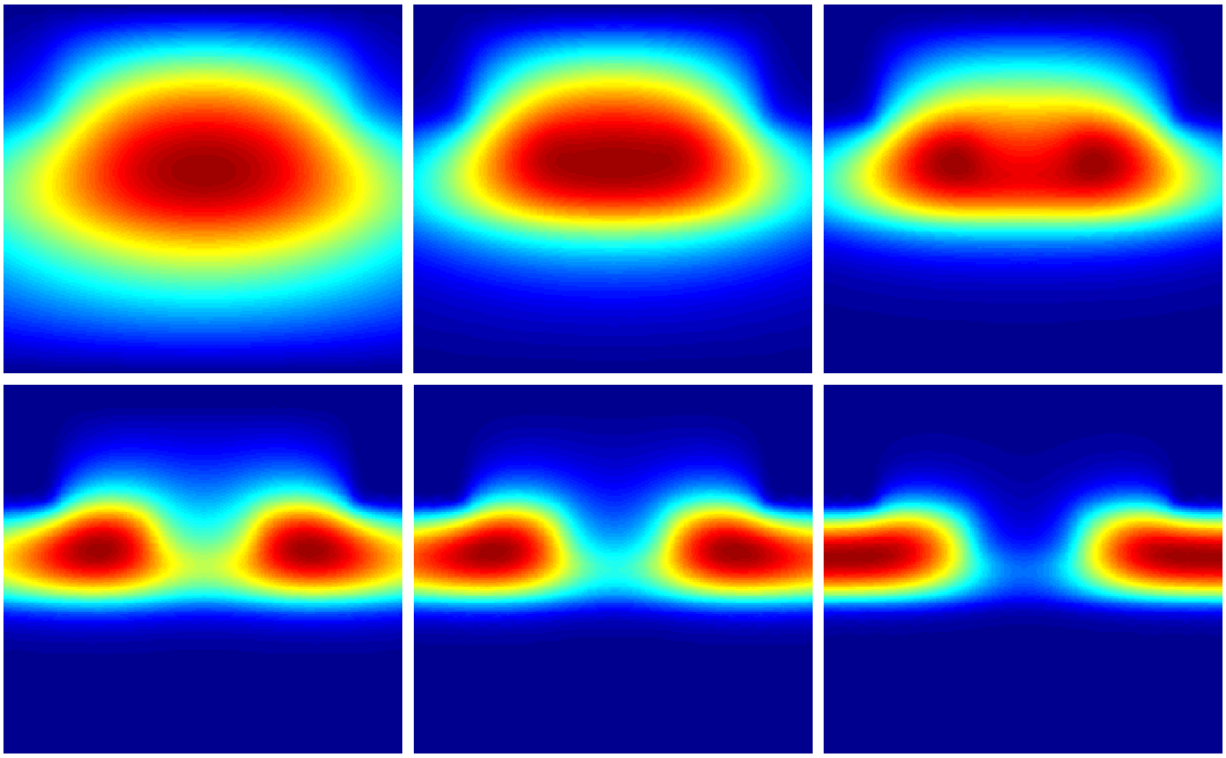

Figure 20: Example 3 - First symmetrized eigenvector for $k = 1, 2, 3, 5, 6, 8$.

The method is described and tested for a stratified medium with three layers. For a greater number of layers, we need to determine the eigenpairs of the one-dimensional problem studied in section 2, with the same steps of calculation.

The scalar equation studied here is the weak guidance approximation of Maxwell system. The vectorial problem presents other difficulties to write an exact condition on the lateral boundary. Indeed, using potentials, the Maxwell system leads to three scalar equations similar to the one studied here [11], and so three series expansion to combine for getting a condition with the vectorial unknown.

References

[1] A.S. Bonnet, *Analyse mathématique de la propagation de modes guidés dans les fibres optiques*, PhD thesis, University Paris 6, April 1988.

[2] A.S. Bonnet-BenDhia, G. Caloz and F. Mahé, *Guided modes of integrated optical guides. A mathematical study*, IMA Journal of Applied Mathematics **60** (1998) 225-261.

[3] A.S. Bonnet-BenDhia, G. Caloz, M. Dauge and F. Mahé, *Study at high frequencies of a stratified waveguide*, to appear.

[4] A.S. Bonnet-BenDhia and N. Gmati, *Spectral approximation of a boundary condition for an eigenvalue problem*, SIAM J. Numer. Anal. **32** (1995) 1263-1279.

[5] A.S. Bonnet-BenDhia and P. Joly, *Mathematical analysis of guided water waves*, SIAM J. Appl. Math. **53** (1993) 1507-1550.

[6] A.S. Bonnet-BenDhia and F. Mahé, *A guided mode in the range of the radiation modes for a rib waveguide*, Journal of Optics **28** (1997) 41-43.

[7] N. Gmati, *Guidage et diffraction d'ondes en milieu non borné*, PhD thesis, University Paris 6, February 1992.

[8] A. Jami and M. Lenoir, *A variational formulation for exterior problems in linear hydrodynamics*, Computer Methods in Applied Mechanics and Engineering, Vol. 16, p. 314-359, 1978.

[9] M. Koshiba, *Optical waveguide theory by the finite element method*, KTC Scientific Publishers, Tokyo, 1992.

[10] M. Lenoir and A. Tounsi, *The localized finite element method and its applications to the two-dimensional sea-keeping problem*, SIAM J. Numer. Anal. **25** (1988) 729-752.

[11] F. Mahé, *Etude mathématique et numérique de la propagation d'ondes électromagnétiques dans les microguides de l'optique intégrée*, PhD thesis, University Rennes I, December 1993.

[12] D. Martin, *Guide d'utilisation du code Mélina*, IRMAR, University Rennes 1 (1997) - `http://www.maths.univ-rennes1.fr/~dmartin`.

[13] B.M.A. Rahman and J.B. Davies, *Finite-Element Analysis of Optical and Microwave Waveguide Problems*, IEE Transactions on Microwave Theory and Techniques, Vol. MTT-32, No. 1, January 1984.

[14] M. Reed and B. Simon, *Analysis of Operators*, Vol. IV, Academic Press, New York, 1978.

[15] A.W. Snyder and J.D. Love, *Optical waveguide theory*, Chapman and Hall, London, 1983.

[16] M. Schechter, *Spectra of partial differential operators*, North-Holland, 1971.

[17] C. Vassalo, *Théorie des guides d'ondes électromagnétiques*, Tomes 1 et 2, Eyrolles Editions and CNET-ENST, Paris, 1985.

[18] J.H. Wilkinson, *The Algebraic Eigenvalue Problem*, Clarenton Press, Oxford, 1965.